

S.Yu. Medvedey¹, A.A. Martynov¹, L. Villard²

¹*Keldysh Institute, Russian Academy of Sciences, Moscow, Russia*

²*Ecole Polytechnique Fédérale de Lausanne (EPFL), Centre de Recherches en Physique des Plasmas, Association Euratom-Confédération Suisse, Lausanne, Switzerland*

The MHD_N0 axisymmetric stability code [1, 2] has been extended to kink mode stability computations. The MHD_NX code computes the ideal MHD stability of plasma equilibrium configurations with arbitrary topology of axisymmetric magnetic surfaces, including doublets, reversed current tokamak configurations with axisymmetric magnetic islands (current holes and AC operation [3, 4]) and multi-connected plasmas like two separated plasma columns (droplet) surrounded by a vacuum region and a conducting wall. The code uses unstructured triangular grids with a possibility of adaptation to the magnetic surfaces and sharp solution features.

The code verification for standard test cases is presented. The results of stability calculations of unconventional tokamak equilibria against the ideal MHD modes with toroidal wave numbers $n = 0$ and $n > 0$ are discussed.

1 Ideal MHD stability: the problem formulation for $n > 0$

For the stability analysis the potential and kinetic energy functionals can be expressed in terms of the electric field perturbation $\vec{E} = i\omega\vec{e}$, $\vec{e} = -\vec{\xi} \times \vec{B}$ (time dependence $e^{i\omega t}$ is assumed for the eigenvalue problem):

$$W_p = \frac{1}{2} \int \left\{ |\nabla \times \vec{e}|^2 - \frac{\vec{j} \cdot \vec{B}}{B^2} \vec{e} \cdot \nabla \times \vec{e} + \frac{\vec{j} \cdot \vec{e}}{B^2} [2\vec{B} \cdot \nabla \times \vec{e} - \vec{t} \cdot \vec{e}] \right\} d^3r, \quad (1)$$

$$K_p = \frac{1}{2} \int \rho |\vec{e}|^2 / B^2 d^3r, \quad \vec{t} = \vec{j} + B^2 \nabla \left(\frac{1}{B^2} \right) \times \vec{B}, \quad (2)$$

combined with the requirement $(\vec{e} \cdot \vec{B}) = 0$, where $\vec{B} = \nabla \psi \times \nabla \phi + F \nabla \phi$ is the equilibrium magnetic field. The surrounding vacuum region (free boundary) can also be taken into account (see [1]). For the force-free case the last term in the functional (1) vanishes because for the equilibrium current density the following representation is valid: $\vec{j} = \vec{j}_{||} + p'(R^2 \nabla \phi - f/B^2 \vec{B})$, $\vec{j}_{||} = (\vec{j} \cdot \vec{B})/B^2 \vec{B}$, so that $\vec{j} \cdot \vec{e} = p' R^2 \vec{e} \cdot \nabla \phi$. An alternative representation for \vec{t} follows from $\vec{t} = -\vec{j} - 2(\vec{B} \nabla \vec{B}) \times \vec{B}/B^2 + 2\vec{j}_{||}$.

The approach to approximate and solve the stability problem on triangular grids includes:

- different finite elements for the longitudinal e_ϕ and poloidal \vec{e}_{pol} projections of the unknown vector $\vec{e} = e_\phi \nabla \phi + \vec{e}_{pol}$: standard node-based "hat"-functions W_i for e_ϕ , and edge-based Whitney elements \vec{W}_{mn} , $\vec{W}_{mn} = W_m \nabla W_n - W_n \nabla W_m$ for \vec{e}_{pol} ;
- Lagrange multipliers introduced to approximate the constraint $(\vec{e} \cdot \vec{B}) = 0$ at each grid node in the plasma region;
- solution of the saddle point matrix eigenvalue problem.

A crucial point is the approximation of the constraint $(\vec{e} \cdot \vec{B}) = 0$. In particular, introducing a small regularizing term into the Lagrange multiplier formulation helps to get robust LU decomposition of the saddle point matrices with standard sparse matrix reordering.

For toroidal harmonics $\vec{e}_n e^{in\phi}$ the $\nabla \times$ operator writes:

$$\nabla \times \vec{e} = e^{in\phi} (\nabla e_{n,\phi} \times \nabla \phi + in \nabla \phi \times \vec{e}_{n,pol} + \nabla \times \vec{e}_{n,pol}).$$

For $n \neq 0$ the harmonic amplitude \vec{e}_n becomes complex and a complex matrix solver is needed. In the MHD_NX code the direct solver from the PETSc package is used, which is available both in real and complex versions. Visualization of the complex solution requires a choice of phase in toroidal angle. It is convenient to preserve a symmetry/anti-symmetry of the real and imaginary parts of the solution eigenvector in case of up-down symmetric equilibrium. An easy way to provide such a normalization of a complex solution is to impose orthogonality between the real and imaginary parts of the solution vector in the scalar product associated with the kinetic energy functional. It gives the following condition on the complex normalization constant c for a given vector of solution x with the use of the scalar product (\cdot, \cdot) :

$$(cx + c^* x^*, cx - c^* x^*) = c^2(x, x) - (c^*)^2(x, x)^* = 0, \quad (c^*/c)^2 = (x, x)/(x, x)^* = e^{i\phi_x}.$$

Then $c = e^{i\phi_c}$ with $\phi_c = -\phi_x/4 + \pi k/2$ is the required normalization constant.

2 Kink mode stability on unstructured grids

Analytic Solovev equilibria were used to run the standard series of the ideal MHD code benchmarks [5]. Two kinds of grids were compared: isotropic unstructured grids, and triangulated structured grids aligned to magnetic surfaces as used in the KINX code [6]. For the fixed boundary mode the results of $n = 2$ stability calculations are shown in Table 1. Due to the absence of displacement projection along the equilibrium magnetic field in the MHD_NX code, the comparative KINX runs were performed for the specific heat ratio $\Gamma = 0$. Note that the MHD_NX convergence is much faster on aligned grid for the internal mode localized near the rational surface $q = 1$ inside plasma. The mode structure is shown in Fig.1. Here the color contours represent the toroidal projection of the electric field $\vec{e} \cdot \nabla \phi / |\nabla \phi| = |\nabla \phi| \vec{\xi} \cdot \nabla \psi$ proportional to the plasma displacement normal to magnetic surfaces. The streamlines are for the displacement vector $\vec{\xi}$.

N	MHD_NX unstructured	N	MHD_NX aligned	KINX
10185	0.135	4097	0.2103	0.2241
40433	0.187	16385	0.2212	0.2258

Table 1. Normalized eigenvalues $-q_1^2 \omega^2 / \omega_A^2$ for fixed boundary $n = 2$ mode. Solovev equilibrium $\epsilon = 1/3$, $E = 2$, the values of safety factor at the magnetic axis and the plasma boundary: $q_0 = 0.7$, $q_1 = 1.22$; N is the number of grid nodes.

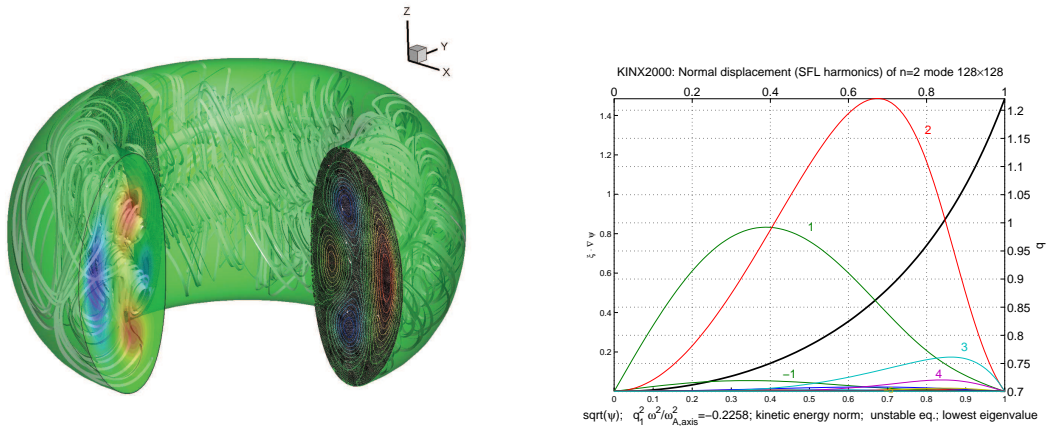


Figure 1. Internal $n = 2$ mode structure. MHD_NX code on unstructured grids and harmonics of the normal plasma displacement.

The convergence is even faster on unstructured grids for the external $n = 1$ kink mode (Table 2). However, the results depend on grid uniformity across the plasma-vacuum interface. It is a general fact that the approximation in the MHD_NX code is quite sensitive to the grid irregularities. This is to be certainly overcome in order to get advantages from the grid adaptation.

N	MHD_NX unstructured	N	MHD_NX aligned	KINX
5929	0.7400	8193	0.7248	0.7883
23865	0.7710	32769	0.7803	0.7930

Table 2. Normalized eigenvalues $-q_1^2 \omega^2 / \omega_A^2$ for free boundary $n = 1$ mode. Solovev equilibrium $\varepsilon = 1/3$, $E = 2$, $q_0 = 1.2$, $q_1 = 2.09$. The conducting wall radius $b/a = 2$.

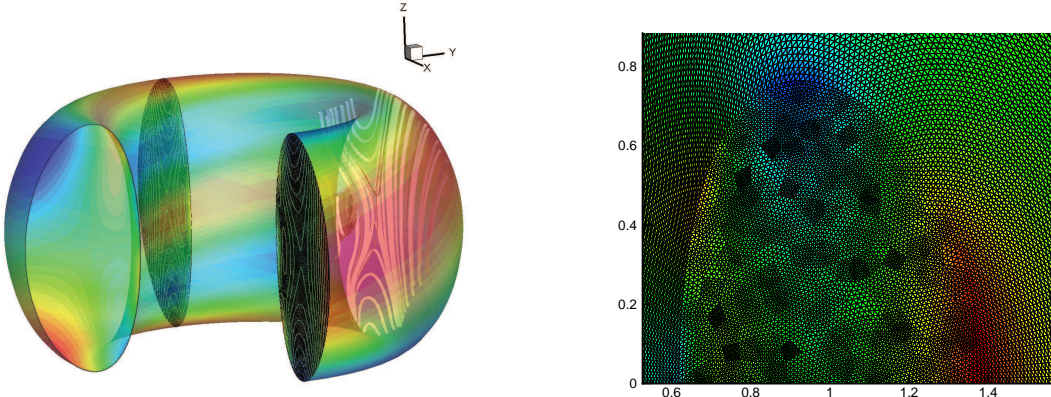


Figure 2. External $n = 1$ mode structure in plasma. The grid in plasma and vacuum regions is also shown in (R, Z) plane.

3 MHD stability with axisymmetric islands

The kink mode structure for an equilibrium with current reversal is presented in Fig.3. The streamlines are for the poloidal projection of the displacement vector $\vec{\xi}$. The large squareness of the cross-section provides the axisymmetric $n = 0$ stability with conducting wall at the plasma boundary (fixed boundary condition) [3]. For sufficiently large negative current fixed boundary $n = 1$ kink mode becomes unstable. It happens before but close to the destabilization of the $n=1$ external mode for the core plasma due to proximity to the Kruskal-Shafranov current limit. Profiles in the core (within the black line in Fig.3) are shown in Fig.4. Due to low $q_0 = 0.21$

and presence of the resonant surfaces $q = 1/n$, $n = 2, 3, 4$, corresponding internal modes are also unstable there. As noted above, the MHD_NX needs the aligned grids for accurate internal mode stability calculation (Fig.4).

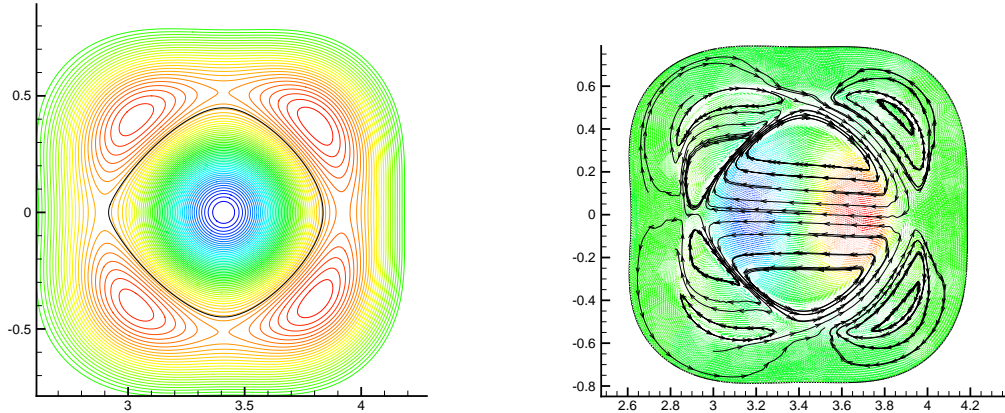


Figure 3. Level lines of the equilibrium poloidal flux for the reversed current equilibrium ($n = 0$ mode is stable with fixed boundary) and the structure of unstable $n = 1$ fixed boundary mode for sufficiently large negative current in the core.

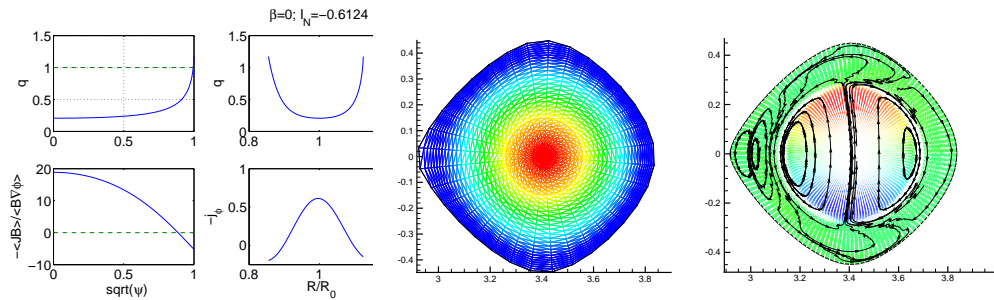


Figure 4. Plasma profiles within the negative current core (black curve in Fig.3, left) and the structure of unstable $n = 3$ fixed boundary mode computed on the grid aligned to magnetic surfaces.

4 Discussion

MHD stability calculations on adaptive unstructured grids provide a powerful tool for high resolution stability analysis. For example, it would be useful for high- n edge localized kink-balloon modes associated with Type-I ELM trigger in divertor geometry. Development of nonlinear MHD code on unstructured grids including finite resistivity, reconnections and 3D islands is an attractive perspective. However, more studies are needed to improve the approximation on irregular grids and increase the accuracy on the grids not aligned to magnetic surfaces.

- [1] A.A.Martynov, S.Yu.Medvedev, L.Villard, Axisymmetric Mode Stability in Tokamaks with Reversed Current Density, 33rd EPS Conf. on Plasma Phys., Rome, Italy, 19 - 23 June 2006, ECA Vol.30I, P-1.167 (2006)
- [2] A.A.Martynov, S.Yu.Medvedev, L.Villard, Tokamaks with Reversed Current Density: Current Holes, AC Operation and Axisymmetric Stability, 34th EPS Conf. on Plasma Phys., Warsaw, Poland, 2 - 6 July 2007, ECA Vol.31F, P-4.087 (2007)
- [3] A.A.Martynov, S.Yu.Medvedev, L.Villard, Tokamaks with Reversed Current Density: Stability of Equilibria with Axisymmetric Islands, 35th EPS Conference on Plasma Phys. Hersonissos, 9 - 13 June 2008 ECA Vol.32D, P-2.063 (2008)
- [4] S.Yu.Medvedev, Y.Hu, A.A.Martynov, L.Villard, Tokamak Plasma Equilibria and Axisymmetric Stability with a Zero Total Toroidal Current, 36th EPS Conference on Plasma Phys. Sofia, June 29 - July 3, 2009 ECA Vol.33E, P-1.130 (2009)
- [5] M.S. Chance *et al.* J. Comput. Phys. **28** (1978) 1-13
- [6] L. Degtyarev *et al.* Comput. Phys. Comm. **103** (1997) 10-27